Published in final edited form as:
Hepatology. 2011 February ; 53(2): 548–557. doi:10.1002/hep.24047.

Combination of retinoic acid and ursodeoxycholic acid attenuates liver injury in bile duct ligated rats and human hepatic cells

Hongwei He*, **Albert Mennone**, **James L. Boyer**, and **Shi-Ying Cai**
Department of Internal Medicine and Yale Liver Center, Yale University School of Medicine, New Haven, CT 06520

Abstract

Cholestasis leads to liver cell death, fibrosis, cirrhosis, and eventually liver failure. Despite limited benefits, ursodeoxycholic acid (UDCA) is the only FDA approved treatment for cholestatic disorders. Retinoic acid (RA) is a ligand for nuclear receptors, which modulate bile salt homeostasis. RA also possesses immunomodulatory effects and is used to treat acute promyelocytic leukemia, and inflammatory disorders such as psoriasis, acne, and rheumatoid arthritis. To test whether supplementation of RA with UDCA is superior to UDCA alone for treating cholestasis, male Sprague-Dawley rats underwent common bile duct ligation (BDL) for 14 days and were treated with PBS, UDCA, all-trans RA (atRA), or UDCA+atRA by gavage. UDCA +atRA treatment substantially improved animal growth rate, significantly reduced liver fibrosis and bile duct proliferation, and nearly eliminated liver necrosis after BDL. Reductions in bile salt pool size and liver hydroxyproline content were also seen with atRA and atRA+UDCA treatment when compared with PBS and UDCA. Further, atRA+UDCA significantly reduced liver mRNA and/or protein expression of Tgf-β1, Col1A1, Mmp2, Ck19, α-Sma, Cyp7a1, Tnf-α and IL-β1. The molecular mechanisms of this treatment were also assessed in human hepatocytes, hepatic stellate cells and LX-2 cells. AtRA alone or in combination with UDCA greatly repressed CYP7A1 expression in human hepatocytes, and significantly inhibited COL1A1, MMP2, and α-SMA expression and/or activity in primary human hepatic stellate cells and LX-2 cells. Furthermore, atRA reduced TGF-β1 induced Smad2 phosphorylation in LX-2 cells. Our findings indicate that the addition of RA to UDCA reduces bile salt pool size and liver fibrosis, and might be an effective supplemental therapy with UDCA for cholestatic diseases.

Keywords

cholestasis; bile acids; liver necrosis, inflammation, fibrosis; combination treatment

Chronic cholestasis results in liver fibrosis, cirrhosis, and eventually liver failure and the need for liver transplantation in disorders such as primary biliary cirrhosis (PBC) and primary sclerosing cholangitis (PSC). Currently, ursodeoxycholic acid (UDCA) is the only effective treatment for PBC, but is limited to early stages of the disease(1). In contrast,

Correspondence: Shi-Ying Cai, Ph.D., Liver Center, Yale University School of Medicine, 333 Cedar Street, 1080 LMP, New Haven, CT 06520. Tel: (203)785-3150; Fax: (203)785-7273; shi-ying.cai@yale.edu. James L. Boyer, M.D. Ensign Professor of Medicine, Emeritus Director, Liver Center, Yale University School of Medicine, 333 Cedar Street, 1080 LMP, New Haven, CT 06520-8019. Phone: (203)785-5279; Fax: (203)785-7273; james.boyer@yale.edu.
*current address: Department of Oncology, Institute of Medicinal Biotechnology, Peking Union Medical College, Chinese Academy of Medical Sciences, Beijing 100050, China

Disclosure: All authors have nothing to disclose.

UDCA is of limited or no benefit for patients with PSC and may even be harmful when given at high dose (25–30 mg/kg)(2). Although much has been learned in recent decades about the molecular basis of cholestasis and the pathophysiology of hepatic fibrosis, new therapeutic approaches have been limited(3). Alternative therapies have been tried but have not been successful based on limited clinical trials, including combinations of UDCA with immunomodulating drugs(4). Thus there is an urgent need to develop alternative beneficial treatments for these chronic cholestatic diseases(5;6).

Retinoic acid (RA), a metabolite of vitamin A, is an agonist for the nuclear receptors RARs and RXRs and is involved in many biological processes, including cell proliferation, differentiation, and morphogenesis. RA also has immunomodulatory and anti-inflammatory effects and inhibits the expression of pro-inflammatory cytokines including TNF-α, IL-1β, and IL-6 in various cell types(7). RA is currently in therapeutic use as an FDA-approved treatment for acute promyelocytic leukemia and inflammatory disorders such as psoriasis, acne, and rheumatoid arthritis(8). In addition, RA is known to inhibit activation of isolated rat hepatic stellate cells (HSC)(9–11). However, this observation has not been verified in human HSCs. All-trans RA (atRA) has also been reported to have anti-fibrotic effects in bile duct ligated (BDL) rats, but the molecular mechanisms remain to be elucidated(12).

Recently we reported that RA can repress CYP7A1 expression in HepG2 cells and in primary human hepatocytes(13). CYP7A1 is the rate-limiting enzyme in converting cholesterol into bile acids. We also observed that UDCA and atRA had synergistic effects in promoter reporter assays in activating FXR and PXR. Therefore, we hypothesized that supplementation of UDCA with RA might be superior to UDCA alone for therapy in cholestatic disorders. In this report, we tested this hypothesis *in vivo* in a BDL rat model of cholestasis and *in vitro* in primary human hepatocytes, HSCs, and LX-2 cells. Our findings support the hypothesis and suggest that the addition of atRA to standard therapy with UDCA might enhance the effectiveness of treatment for chronic cholestatic disorders likely by reducing bile acid synthesis and pool size and blocking profibrotic TGF-β signaling pathways.

Materials and Methods

Materials

Chemicals were purchased from Sigma (St. Louis, MO), except where otherwise specified. Cell culture media DMEM and IMDM, fetal bovine serum (FBS), penicillin/streptomycin, trypsin and phosphate buffered saline (PBS) were from Invitrogen (Carlsbad, CA). HMM medium is from Lonza (Walkersville, MD). Matrigel was purchased from BD Sciences (Bedford, MA). TGF-β1 (240-B) was purchased from R&D Systems (Minneapolis, MN).

Animal experiments

All animal experimental protocols were approved by the local Animal Care and Use Committee, according to criteria outlined in the “Guide for the Care and Use of Laboratory Animals” prepared by the National Academy of Sciences, as published by the National Institutes of Health (NIH publication 86–23, revised 1985). Male Sprague-Dawley rats (200–230 g) were obtained from Charles River (Wilmington, MA). For experiments with BDL, rats were randomly divided into five groups, with each containing up to seven animals. Each day, four animals underwent BDL together with a sham operated animal as a healthy control. Twenty-four hours post-surgery, the four BDL animals were randomly assigned to receive daily gavages consisting of either PBS (the treatment control and solvent), 15mg/kg UDCA (suspended in PBS), 5mg/kg atRA, or UDCA (15mg/kg) supplemented with atRA (5mg/kg), all for 14 days. The sham controls also received PBS by

gavage. BDL rats also received 0.5 mg vitamin K qod by subcutaneous injection. Body weight was measured daily. The animals were sacrificed in random order between 9:00 am – 11:00 am after an overnight fast. Samples of serum, bile (from bile duct cyst in BDL animals), urine (from bladder), liver, kidney, and ileum (10 cm) were collected for further analyses.

Serum biochemistry and liver histology

Serum total bilirubin, aminotransferase (ALT), and γ–glutamyl-transpeptidase (GGT) were analyzed using kits from Thermo Fisher Scientific (Cincinnati, OH). Serum levels of total cholesterol and HDL were determined by the Analytical Core, Mouse Metabolic Phenotyping Center at Yale University. Bile salt (3α-hydroxy bile salt) concentrations in serum, bile, urine and liver tissue were determined using a kit from Trinity BioTech (Newark, NJ). The bile salt pool size was calculated by adding measurement of bile salt content in bile, liver and serum (normalized to body weight) (assuming serum as 7.6% of the body weight). Formalin fixed tissue was embedded in paraffin and sections were stained with hematoxylin and eosin, and Sirius Red. Liver histology was blindly assessed for inflammation, necrosis, bile duct proliferation and fibrosis on a 1–4+ scale. Liver hydroxyproline content was measured as described(14).

Cells isolation and maintenance

All cells were maintained at 37°C in a humidified atmosphere containing 5% CO_2. Both human hepatocytes and hepatic nonparenchymal cell fractions were obtained from the Liver Tissue Procurement and Distribution System of the NIH (Dr. Stephen Strom, University of Pittsburgh). Human hepatocytes were maintained as described(13). Human HSCs were isolated from the nonparenchymal cell fraction using 11% Nycodenz gradient centrifugation as previously described(15;16). Isolated HSCs were cultured in plastic plate/flasks with IMDM medium supplemented with 20% FBS and 0.06 μM insulin, 0.1 mM nonessential amino acids, 1 mM sodium pyruvate, and antibiotic/antifungi solution. When 100% confluence was nearly reached, the primary cultures were always split at 1:3 for each passage. Passage 1 cells were characterized by immunofluorescence staining using human HSC specific markers, including α-SMA, Vimentin, COL I, and Vinculin(17). All the experiments and phenotype tests were performed using cells from passages 1 to 5. Before treatment, cells were serum starved for 24h in IMDM. LX-2 cells were a gift from Dr. Scott Friedman (Mount Sinai Medical Center, New York) and maintained in DMEM containing 10% FBS, 1% penicillin/streptomycin. At 50–70% confluence, LX-2 cells were starved in serum-free DMEM for 24h, prior to treatment with TGF-β1 and/or atRA in serum-free DMEM.

Gelatin Zymography

MMP-2 and -9 gelatinase activity was detected as described(18). Briefly, media (30 μl) from the same number of cells with different treatments were electrophoresed at 4 °C in 8% SDS–PAGE containing 1 mg/ml of gelatin. After electrophoresis, the gel was washed, developed, and stained with 0.5% Coomassie Blue R-250. After destaining with water, the gel was scanned using Odyssey (Li-Cor) and the band intensity was quantified.

Immunofluorescence staining and confocal microscopy

Cells were fixed in 4% paraformaldehyde and permeabilized by methanol. After blocking, the cells were incubated overnight with anti-Smad2 (1:400) (Cell Signaling Technology). The secondary antibody was labeled with FITC. Nuclei were stained using Topro-3. Fluorescent images were taken using a Zeiss LSM 510 confocal microscope.

Quantitative real-time PCR and Western blot analysis

As described in(13), gene mRNA expression was detected using TaqMan real-time PCR in an ABI7500 system and protein was analyzed by Western blotting. GAPDH gene was used as reference to normalize data. The TaqMan primer/probe and antibodies are listed in Table S2 and S3, respectively.

Statistical Analysis

Data are expressed as means ± standard deviation (SD). Differences between experimental groups were assessed for significance using the two-tailed Student *t*-test. A p value of < 0.05 was considered to be statistically significant.

Results

UDCA supplemented with atRA improved growth rate, liver gross appearance and reduced bile duct cyst size in BDL rats

The growth rates of 14 day BDL animals treated with PBS, UDCA or atRA (Group 2–4, respectively) were significantly lower than the sham group (Group 1) as expected in animals undergoing BDL. In contrast, the growth of animals treated with UDCA supplemented with atRA (Group 5) although slightly less was not significantly different from the sham group (Table 1A), suggesting that this treatment improved the overall condition of these cholestatic animals. This beneficial effect was also noted in the gross appearance of the liver at sacrifice where livers from animals in Group 2 had a rough cirrhotic appearance to their surface. In contrast, Group 5's liver surface had a smooth and shiny appearance similar to Group 1 (Figure 1A). The appearance of the liver surface of Group 3 was similar to Group 2's, while the surface of animals in Group 4 was closer to Group 5. In addition, the relative weight of the livers of Group 5 was significantly smaller than Groups 2 and 3. Smaller livers were also seen in Group 4 (Table 1A). Notably, the size of the bile duct cyst (volume of bile) from the livers of Group 5 was significantly smaller than from Group 2 and 3 (Table 1A), suggesting that less bile was produced in these animals. There were no significant changes in kidney weight among the BDL groups. As expected, serum ALT and GGT levels were significantly higher in BDL groups than in the sham controls. Interestingly, ALT levels were further increased in Group 5, whereas lower GGT levels were seen in Group 4. There were no significant differences in serum bile salt levels among the BDL animals although higher serum bilirubin levels and lower serum cholesterol levels were detected in Group 5.

Combination treatment with atRA and UDCA markedly reduced hepatic bile salt levels and the bile salt pool size in BDL rats

While bile salt concentrations in liver tissues and urine were increased in all BDL groups, the total amount of bile salts in the liver and bile cysts of Group 4 and 5 were lower. Further, estimates of the total bile salt pool revealed significantly lower levels in Groups 4 and 5 when compared to Groups 2 and/or 3 (Table 1B).

Combination treatment with atRA + UDCA improved liver histology in BDL rats

BDL in rats is associated with significant increases in liver fibrosis and bile duct proliferation as confirmed by H&E and Sirius Red staining of liver tissue when scored without knowledge of treatment. However, Group 4 and 5 had significantly less liver fibrosis and bile duct proliferation (Figure 1B, C). Blinded assessment also revealed significantly lower scores for necrosis in Group 4 and 5 with the lowest scores in Group 5. There was no significant histological difference in inflammation among the BDL groups (Figure 1B, C).

AtRA alone or in combination with UDCA reduced the expression of marker genes for liver fibrosis, duct proliferation, and inflammation in BDL rats

Hydroxyproline analysis revealed significantly lower levels of this fibrosis marker in the livers of Group 4 and 5 when compared to Group 2 and 3 (Figure 2A), in agreement with the assessment of hepatic histology. Of particular note, hydroxyproline content in Group 5 was reduced to levels similar to Group 1. This suggests that addition of atRA to UDCA therapy greatly reduces the stimulus for fibrosis formation in this rat model of cholestasis.

This notion is supported by gene expression analyses. As illustrated in Figure 2B, mRNA expression of Tgf-β1, Collagen1a1, matrix metalloproteinase-2 (Mmp-2) and Ck19 were significantly reduced in the livers in Group 5 and/or 4. Western blot analysis revealed significant reduction in α-Sma protein expression in the livers of Group 5 when compared to other BDL groups (Figure 2C).

Although assessment of liver histology did not reveal differences in inflammation among BDL groups, real-time PCR did detect significant reductions in the mRNA expression of inflammatory cytokines (TNF-α and IL-1β), which were particularly noted in Group 5 animals (Figure 2D).

Combination treatment with atRA + UDCA significantly repressed Cyp7a1 expression in BDL rat livers

To investigate the mechanism of the reduced bile acid pool size in UDCA and atRA treated rats, we analyzed the expression of genes involved in bile acid synthesis and transport in the liver, ileum and kidneys. Figure 3A demonstrates that hepatic Cyp7a1 mRNA expression was significantly reduced in Group 5 (33% of the level of Group 2), whereas hepatic Shp was increased ~ 3-fold in Group 5 despite reductions in Fxr (Nr1h4). Hepatic Fgf15 mRNA expression was also increased in all BDL groups. These findings confirm the reciprocal relationship between expression of Cyp7a1 and Shp/Fgf15(19), and may partially explain the reduced bile acid pool size in Group 5 rats.

Assessment of the expression of bile acid transporters and other bile acid regulatory proteins revealed no substantial differences in the mRNA and/or protein expression among BDL groups, whereas increased hepatic Mrp3 but decreased Ntcp and Mrp2 expression were seen in all BDL groups compared to sham control (Table S1 and data not shown).

There were no substantial changes in ileal Fxr or Ostα mRNA expression, although the ileal Asbt (Slc10a2) mRNA levels in Group 5 were slightly but significantly lower than Group 2 (68.8% of the control) (Table S1). As bile acids were excluded from the intestine of BDL rats, substantial reductions in ileal Fgf15 mRNA expression were detected in these animals compared to sham controls, but there was no significant difference between Group 3 and 5.

In the kidney, BDL resulted in increased mRNA expression of Ostα, Ostβ and Mrp4 as previously described(20), but the difference between Group 3 and 5 was not significant (Table S1).

AtRA +/− UDCA inhibits CYP7A1 expression in human hepatocytes

To verify whether UDCA and atRA can synergistically inhibit bile acid synthesis in human cells, we treated human hepatocytes with atRA and/or UDCA. Compared to the solvent control, 50 μM UDCA, 1 and 5 μM atRA, reduced CYP7A1 mRNA expression levels to about 40%, 2%, and <2%, respectively (Figure 3B). Combination of UDCA and atRA (1 or 5 μM) further decreased the levels to <1% of the control. Increased SHP and FGF19 expressions were also seen with these treatments, whereas FXR, BSEP, MRP4, and

CYP3A4 mRNA were unchanged. This result demonstrates that atRA with or without UDCA can repress the expression of CYP7A1 in human hepatocytes.

AtRA reduced Col1A1 and MMP2 expression in primary human HSCs and LX-2 cells independent of UDCA

As atRA alone or in combination with UDCA reduced markers of hepatic fibrosis in BDL rats, we next examined if this therapy would have similar anti-fibrotic effects in a human HSC line, LX-2 cells. Fig 4A demonstrates that 24 hrs treatment with 5 μM atRA significantly repressed TGF-β1 activation of COL1A1 mRNA expression by nearly 50%, while a modest reduction in MMP2 mRNA expression was also detected. In contrast, UDCA (50 μM) alone had no significant effect on the expression of these two genes (data not shown). The combination of atRA with UDCA yielded essentially the same results as atRA treatment alone (data not shown). Pro-collagen α1(I) and α-SMA protein expression by Western blot was also reduced in these cells after atRA treatment (Figure 4B). In addition 5 μM atRA significantly reduced MMP2 enzymatic activity after TGF-β1 stimulation, as assayed by zymography using LX-2 culture medium. In contrast, MMP9 was not changed by these treatments (Figure 4C).

The anti-fibrotic effect of atRA was further verified in primary human HSCs. Figure 4D demonstrated that 5 μM atRA alone or in combination with 50 μM UDCA significantly repressed COL1A1 mRNA expression by more than 50% in these cells, where a reduction in MMP2 expression was also seen. As in LX-2 cells, 50 μM UDCA alone did not show any effect in these primary human HSCs either. However, in contrast to LX-2 cells, addition of 2 ng/ml TGF-β1 to the medium of these activated primary human HSCs did not further stimulate COL1A1 expression (data not shown). Of note, COL1A1 mRNA expression increased by > 650-fold when comparing cultures from day 1 to day 10 after isolation. Together, these results indicate that atRA exerts its anti-fibrotic effects in the liver by repressing COL1A1, α-SMA and MMP2 expression.

AtRA reduced Smad2 phosphorylation in TGF-β1 stimulated LX-2 cells

Phosphorylated Smad2 plays an important role in the activation of TGF-β1 induced COL1A1 expression(21;22). To assess if RA repression of COL1A1 expression is mediated through this pathway, we detected the levels of expression and/or phosphorylation of several proteins involved in the TGF-β1 - Smad2 signaling cascade. Figure 5A demonstrates that atRA (5μM) markedly reduced TGF-β1 induction of Smad2 phosphorylation in LX-2 cells, under conditions where the total amount of Smad2 was not changed. AtRA also decreased the expression of Smad4 in these cells (Fig. 5A), whereas Smad6, Smad7, and TGIF protein expression was either not changed or was undetectable (data not shown). Immunofluorescent labeling also demonstrated that the nuclear localization of Smad2 (presumably the activated phosphorylated form) was greatly diminished after treatment with 5 μM atRA (Figure 5B). These results suggest that atRA's inhibitory effect on COL1A1 expression is mediated by blocking TGF-β1-stimulated Smad2 phosphorylation.

Discussion

In this report, we assessed the therapeutic effects of combining atRA with UDCA *in vivo* in a BDL cholestatic rat model and *in-vitro* in human hepatic cells. We demonstrate that supplementation of atRA (5mg/kg) with UDCA (15mg/kg) has achieved superior effects to UDCA or atRA treatment alone in BDL rats by 1) improving animal growth and liver histology, including reducing bile duct proliferation, necrosis, and fibrosis (Table 1A, Figure 1); 2) reducing liver hydroxyproline content and other inflammatory and fibrotic markers (Figure 2); 3) reducing bile salt pool size (Table 1B). Furthermore, the mechanisms of the

combination treatment were verified in human hepatic cells, including hepatocytes, HSC and LX-2 cells (Figure 3 & 4).

Chronic cholestasis leads to liver necrosis, fibrosis and cirrhosis partially due to accumulation of toxic bile acids in the liver(23). UDCA therapy is based on its properties as a non-toxic hydrophilic bile acid that reduces the hydrophobicity of the bile acid pool, thereby reducing bile salt toxicity(24). In addition, UDCA may act as a transcription factor modulator, for PXR and Nrf2 which regulate the expression of genes involved in bile salt detoxification and redox signaling(25;26). Furthermore, UDCA is known to have anti-apoptotic effects in various cell systems(27;28). However, UDCA does not seem to be an effective modulator of HSC activation, cell proliferation, or immune system pathways. Recent studies even suggest that UDCA may be harmful in obstructive cholestasis by increasing biliary pressure and liver necrosis as shown in mouse models of BDL and when administered in high doses to patients with PSC(2;29). In contrast, RA is not only an activator for nuclear receptors that play a role in maintaining bile salt homeostasis(13;30), but also an immunomodulator whose anti-inflammatory properties are used to treat certain autoimmune diseases(7;8). Because these two compounds have such complimentary properties, we hypothesized that addition of RA to UDCA treatment might improve hepatic function in cholestatic liver diseases to a greater extent than UDCA treatment alone. As seen in this report, this hypothesis is supported by our experimental results.

First, atRA alone or in combination with UDCA greatly repressed CYP7A1/Cyp7a1 expression in BDL rats and human hepatocytes, whereas UDCA alone did not (Figure 3). The reduction of CYP7A1/Cyp7a1 expression may decrease bile acid synthesis and explain reduced bile salt pool size in animals with combination treatment, which should be beneficial in cholestasis. Secondly, the combination treatment significantly decreased the hepatic expression levels of inflammatory cytokines Tnf-α and IL-1β in BDL rats (Figure 2). These observations are consistent with previous reports, where RA's anti-inflammatory effects have been investigated in nonhepatic cells(7). Most importantly, the combination treatment achieved superior effects to UDCA or atRA alone in reducing necrosis, bile duct proliferation and fibrosis in the livers of BDL rats (Figure 1). These findings are further supported by biochemical and gene expression analyses, as markers such as hydroxyproline content, expression of Mmp2, α-Sma, and Ck19 in the livers of the combination treatment were significantly decreased when compared to UDCA or atRA treatment alone (Figure 2). Of note, atRA treatment alone also showed some beneficial effects as reported in other liver injury models(31). However, to our knowledge, RA has never been tested in patients with liver fibrosis. To determine whether human cells would show the same response to RA, we treated human primary HSC and LX-2 cells with atRA and/or UDCA. Once again, UDCA (50 μM) alone did not have beneficial effects and did not alter the expression of COL1A1, MMP2, and α-SMA in contrast to 5 μM atRA alone or in combination with UDCA, findings consistent with the results in the animal studies. Together, these results provide an explanation of atRA's beneficial effects in human liver cells as well as in the rat model of cholestasis.

Additional findings into the mechanism of this antifibrotic effect suggest that atRA suppresses COL1A1 expression via the TGF-β1/Smad signaling pathways. HSCs are the major target of TGF-β1, which help stimulate the transdifferentiation of HSC into fibrogenic myofibroblasts(32). TGF-β1 production, as well as IL-6 are up-regulated in myofibroblasts and proliferating bile duct epithelia after BDL and further contribute to the fibrogenic process in an autocrine/paracrine manner(33). Down stream signaling in HSC involves signaling transcription factors Smads 2, 3, and 4. Based on cell culture studies, TGF-β is thought to mediate activation of Smad2 initially and Smad3 later through phosphorylation and followed by nuclear translocation of these two proteins(34). Here using LX-2 cells, we

find that atRA reduced Smad2 phosphorylation in a dose-dependent manner, where Smad4 protein expression was also decreased while other proteins potentially involved in Smad signaling did not significantly change, including TGIF, Smad6 and Smad7 in LX-2 cells. These findings are consistent with a significant anti-fibrotic effect of atRA mediated through inhibition of the TGF-β1/Smad pathway. It remains to be determined how atRA represses Smad2 phosphorylation.

In summary, we have demonstrated that supplementation of atRA with UDCA improves the therapeutic response and is superior to UDCA treatment alone in a rat model of cholestasis and *in vitro* in human hepatic cells. These findings suggest that addition of atRA to current therapeutic regimens (UDCA) might be beneficial in patients with chronic cholestatic disorders.

Supplementary Material

Refer to Web version on PubMed Central for supplementary material.

Acknowledgments

We thank Kathy Harry and Dr. Carol Soroka for technical assistance. Normal human hepatocytes and nonparenchymal cell fraction were obtained through the Liver Tissue Cell Distribution System, Pittsburgh, Pennsylvania, which was funded by NIH Contract #N01-DK-7-0004 / HHSN267200700004C.

Grant Support: This study was supported by an American Liver Foundation PBC Fund for the Cure (S.Y.C.), and National Institutes of Health Grants DK34989 (Yale Liver Center) and DK25636 (to J.L.B.).

Reference

1. Kaplan MM, Gershwin ME. Primary biliary cirrhosis. N Engl J Med. 2005; 353(12):1261–1273. [PubMed: 16177252]
2. Lindor KD, Kowdley KV, Luketic VA, Harrison ME, McCashland T, Befeler AS, et al. High-dose ursodeoxycholic acid for the treatment of primary sclerosing cholangitis. Hepatology. 2009; 50(3): 808–814. [PubMed: 19585548]
3. Hohenester S, Oude-Elferink RP, Beuers U. Primary biliary cirrhosis. Semin Immunopathol. 2009; 31(3):283–307. [PubMed: 19603170]
4. Silveira MG, Lindor KD. Treatment of primary biliary cirrhosis: therapy with choleretic and immunosuppressive agents. Clin Liver Dis. 2008; 12(2):425–443. [PubMed: 18456189]
5. Chapman R, Fevery J, Kalloo A, Nagorney DM, Boberg KM, Shneider B, et al. Diagnosis and management of primary sclerosing cholangitis. Hepatology. 2010; 51(2):660–678. [PubMed: 20101749]
6. Zein CO, Lindor KD. Latest and emerging therapies for primary biliary cirrhosis and primary sclerosing cholangitis. Curr Gastroenterol Rep. 2010; 12(1):13–22. [PubMed: 20425480]
7. Montrone M, Martorelli D, Rosato A, Dolcetti R. Retinoids as critical modulators of immune functions: new therapeutic perspectives for old compounds. Endocr Metab Immune Disord Drug Targets. 2009; 9(2):113–131. [PubMed: 19519462]
8. Reichrath J, Lehmann B, Carlberg C, Varani J, Zouboulis CC. Vitamins as hormones. Horm Metab Res. 2007; 39(2):71–84. [PubMed: 17326003]
9. Davis BH, Kramer RT, Davidson NO. Retinoic acid modulates rat Ito cell proliferation, collagen, and transforming growth factor beta production. J Clin Invest. 1990; 86(6):2062–2070. [PubMed: 2254460]
10. Pinzani M, Gentilini P, Abboud HE. Phenotypical modulation of liver fat-storing cells by retinoids. Influence on unstimulated and growth factor-induced cell proliferation. J Hepatol. 1992; 14(2–3): 211–220. [PubMed: 1500685]

11. Hellemans K, Verbuyst P, Quartier E, Schuit F, Rombouts K, Chandraratna RA, et al. Differential modulation of rat hepatic stellate phenotype by natural and synthetic retinoids. Hepatology. 2004; 39(1):97–108. [PubMed: 14752828]
12. Wang H, Dan Z, Jiang H. Effect of all-trans retinoic acid on liver fibrosis induced by common bile duct ligation in rats. J Huazhong Univ Sci Technolog Med Sci. 2008; 28(5):553–557. [PubMed: 18846337]
13. Cai SY, He H, Nguyen T, Mennone A, Boyer JL. Retinoic acid represses CYP7A1 expression in human hepatocytes and HepG2 cells by FXR/RXR-dependent and independent mechanisms. J Lipid Res. 2010
14. Soroka CJ, Mennone A, Hagey LR, Ballatori N, Boyer JL. Mouse organic solute transporter alpha deficiency enhances renal excretion of bile acids and attenuates cholestasis. Hepatology. 2010; 51(1):181–190. [PubMed: 19902485]
15. Friedman SL, Rockey DC, McGuire RF, Maher JJ, Boyles JK, Yamasaki G. Isolated hepatic lipocytes and Kupffer cells from normal human liver: morphological and functional characteristics in primary culture. Hepatology. 1992; 15(2):234–243. [PubMed: 1735526]
16. Casini A, Pinzani M, Milani S, Grappone C, Galli G, Jezequel AM, et al. Regulation of extracellular matrix synthesis by transforming growth factor beta 1 in human fat-storing cells. Gastroenterology. 1993; 105(1):245–253. [PubMed: 8514041]
17. Van Rossen E, Vander BS, van Grunsven LA, Reynaert H, Bruggeman V, Blomhoff R, et al. Vinculin and cellular retinol-binding protein-1 are markers for quiescent and activated hepatic stellate cells in formalin-fixed paraffin embedded human liver. Histochem Cell Biol. 2009; 131(3): 313–325. [PubMed: 19052772]
18. Kleiner DE, Stetler-Stevenson WG. Quantitative zymography: detection of picogram quantities of gelatinases. Anal Biochem. 1994; 218(2):325–329. [PubMed: 8074288]
19. Chiang JY. Bile acids: regulation of synthesis. J Lipid Res. 2009
20. Mennone A, Soroka CJ, Cai SY, Harry K, Adachi M, Hagey L, et al. Mrp4−/− mice have an impaired cytoprotective response in obstructive cholestasis. Hepatology. 2006; 43(5):1013–1021. [PubMed: 16628672]
21. Poncelet AC, de Caestecker MP, Schnaper HW. The transforming growth factor-beta/SMAD signaling pathway is present and functional in human mesangial cells. Kidney Int. 1999; 56(4): 1354–1365. [PubMed: 10504488]
22. Trojanowska M. Noncanonical transforming growth factor beta signaling in scleroderma fibrosis. Curr Opin Rheumatol. 2009; 21(6):623–629. [PubMed: 19713852]
23. Svegliati-Baroni G, Ridolfi F, Hannivoort R, Saccomanno S, Homan M, De Minicis S, et al. Bile acids induce hepatic stellate cell proliferation via activation of the epidermal growth factor receptor. Gastroenterology. 2005; 128(4):1042–1055. [PubMed: 15825085]
24. Pusl T, Beuers U. Ursodeoxycholic acid treatment of vanishing bile duct syndromes. World J Gastroenterol. 2006; 12(22):3487–3495. [PubMed: 16773706]
25. Schuetz EG, Strom S, Yasuda K, Lecureur V, Assem M, Brimer C, et al. Disrupted bile acid homeostasis reveals an unexpected interaction among nuclear hormone receptors, transporters, and cytochrome P450. J Biol Chem. 2001; 276(42):39411–39418. [PubMed: 11509573]
26. Kawata K, Kobayashi Y, Souda K, Kawamura K, Sumiyoshi S, Takahashi Y, et al. Enhanced Hepatic Nrf2 Activation After Ursodeoxycholic Acid Treatment in Patients with Primary Biliary Cirrhosis. Antioxid Redox Signal. 2010
27. Bellentani S. Immunomodulating and anti-apoptotic action of ursodeoxycholic acid: where are we and where should we go? Eur J Gastroenterol Hepatol. 2005; 17(2):137–140. [PubMed: 15674088]
28. Amaral JD, Viana RJ, Ramalho RM, Steer CJ, Rodrigues CM. Bile acids: regulation of apoptosis by ursodeoxycholic acid. J Lipid Res. 2009; 50(9):1721–1734. [PubMed: 19417220]
29. Fickert P, Zollner G, Fuchsbichler A, Stumptner C, Weiglein AH, Lammert F, et al. Ursodeoxycholic acid aggravates bile infarcts in bile duct-ligated and Mdr2 knockout mice via disruption of cholangioles. Gastroenterology. 2002; 123(4):1238–1251. [PubMed: 12360485]
30. Repa JJ, Turley SD, Lobaccaro JA, Medina J, Li L, Lustig K, et al. Regulation of absorption and ABC1-mediated efflux of cholesterol by RXR heterodimers. Science. 2000; 289(5484):1524–1529. [PubMed: 10968783]

31. Hisamori S, Tabata C, Kadokawa Y, Okoshi K, Tabata R, Mori A, et al. All-trans-retinoic acid ameliorates carbon tetrachloride-induced liver fibrosis in mice through modulating cytokine production. Liver Int. 2008; 28(9):1217–1225. [PubMed: 18397230]

32. Parola M, Marra F, Pinzani M. Myofibroblast - like cells and liver fibrogenesis: Emerging concepts in a rapidly moving scenario. Mol Aspects Med. 2008; 29(1–2):58–66. [PubMed: 18022682]

33. Dranoff JA, Wells RG. Portal fibroblasts: Underappreciated mediators of biliary fibrosis. Hepatology. 2010; 51(4):1438–1444. [PubMed: 20209607]

34. Liu C, Gaca MD, Swenson ES, Vellucci VF, Reiss M, Wells RG. Smads 2 and 3 are differentially activated by transforming growth factor-beta (TGF-beta) in quiescent and activated hepatic stellate cells. Constitutive nuclear localization of Smads in activated cells is TGF-beta-independent. J Biol Chem. 2003; 278(13):11721–11728. [PubMed: 12547835]

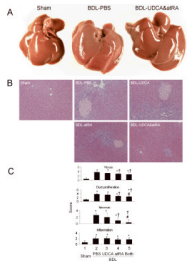

Figure 1.

AtRA supplementation with UDCA markedly improved the liver gross appearance and histology in BDL rats. A, gross liver appearance; B, H & E stained liver histology; and C, Scores of double-blind assessment of liver histology regarding fibrosis (also confirmed by Sirius Red staining), bile duct proliferation, necrosis, and inflammation. $p < 0.05$, n=5–7, * to sham, † to BDL-PBS, # to BDL-UDCA, and & to BDL-atRA. Both = BDL-UDCA&atRA.

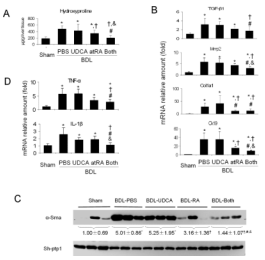

Figure 2.

Biochemical and gene expression analyses. Combination of atRA and UDCA significantly reduced the expression of marker genes for liver fibrosis, bile duct proliferation and inflammation. A, liver hydroxyproline levels; B, liver mRNA expression of TGF-β1, collagen 1a1 (Col1a1), matrix metalloproteinase-2 (Mmp-2), cytokeratin 19 (Ck19); C, liver alpha-smooth muscle actin (α-Sma) protein expression detected by Western blot where data is normalized to house-keeper gene Sh-ptp1; D, liver TNF-α and IL-1β mRNA expression. $p < 0.05$, n=5–7, * to sham, † to BDL-PBS, # to BDL-UDCA, and & to BDL-atRA. Both = BDL-UDCA&atRA.

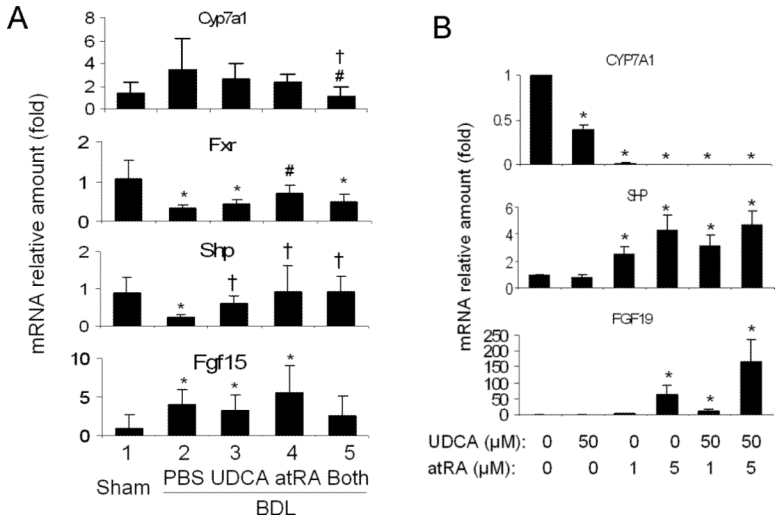

Figure 3.

AtRA supplementation with UDCA synergistically repressed Cyp7a1 mRNA expression *in vivo* in BDL rat livers (A) and great repression of CYP7A1 expression *in vitro* in human hepatocytes by atRA +/− UDCA (B), where increased mRNA expression of SHP/Shp and FGF19/Fgf15 were also detected. For A, $p < 0.05$, n=5–7, * to sham, † to BDL-PBS, # to BDL-UDCA, and & to BDL-atRA. Both = BDL-UDCA&atRA.

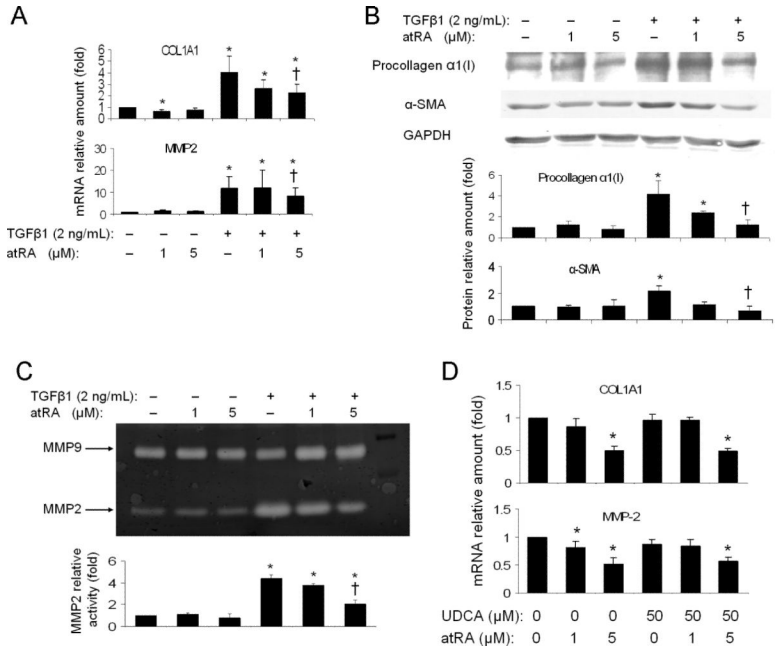

Figure 4.

AtRA alone or in combination with UDCA significantly reduced the expression of fibrotic marker genes in human hepatic stellate cell line LX-2 cells and primary human hepatic stellate cells. A, mRNA expression of collagen 1A1 (COL1A1) and matrix metalloproteinase-2 (MMP-2) in LX-2 cells; B, Western blot analysis of pro-collagen α1 and alpha-smooth muscle actin (α-SMA) expression in LX-2 cells; C, gelatin zymography assay detected reduced MMP-2 expression/activity in the culture medium of atRA treated LX-2 cells; D, atRA decreased mRNA expression of COL1A1 and MMP-2 in human hepatic stellate cells. $p<0.05$, n=3–4, * to medium control, † to 2 ng/ml TGF-β1 treatment control.

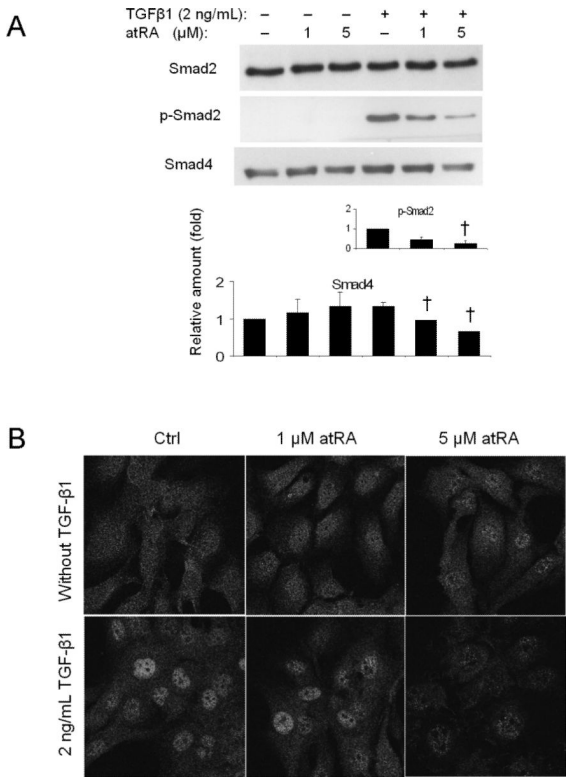

Figure 5.

AtRA significantly reduced TGF-β1 stimulated Smad2 phosphorylation and Smad4 protein expression (A) and Smad2 nuclear translocation (B) in LX-2 cells. $p<0.05$, n=3–4, † to 2 ng/ml TGF-β1 treatment control.

Table 1A

Growth rate, organ weight and serum biochemistry of bile duct ligated (BDL) rats

	Sham-PBS (n=7)	BDL-PBS (n=7)	BDL-UDCA (n=5)	BDL-atRA (n=6)	BDL-UDCA&atRA (n=7)
Growth rate (daily %)	2.65±0.77	1.42 ±0.64[1]	1.43±0.66[1]	1.20±0.42[1]	1.88 ±0.87
Liver/Body weight (g/kg)	30.4±2.3	63.9±7.3[1]	61.6±4.5[1]	48.4±3.3[1,2]	51.6±3.0[1,2,3]
Size of bile cyst (ml/kg)	N/A	5.03±3.06	2.30±0.97	1.53±1.00[2]	1.06±0.54[2,3]
Kidney/Body weight (g/kg)	7.1±0.5	8.8±1.1[1]	9.3±0.6[1]	8.6 ±0.7[1]	8.6 ±0.4[1]
Serum ALT (U/L)	16.12±8.08	35.27±13.55[1]	57.32±15.21[1,2]	41.74±11.65[1]	67.02±23.45[1,2,4]
Serum GGT (U/L)	29.91±23.07	163.16±75.69[1]	129.59±36.47[1]	80.00±27.75[1,2]	143.19±26.83[1]
Serum bile acids (μM)	9.92±5.16	484.43±135.49[1]	511.14±73.20[1]	355.93±181.98[1]	443.80±145.99[1]
Serum bilirubin (mg/L)	0.45±0.15	7.13±2.89[1]	7.25±1.11[1]	5.91±3.26[1]	10.16±2.32[1,3,4]
Serum total cholesterol (mg/L)	66.54±12.52	90.52±20.66[1]	100.74±14.91[1]	88.21±14.94[1]	76.78±9.533

Note:

N/A, not applicable.

[1] p-value < 0.05 to Sham control

[2] to BDL-PBS control

[3] to UDCA treatment

[4] atRA treatment.

Table 1B

Bile salt concentration/amount in rats

	Sham-PBS (n=7)	BDL-PBS (n=7)	BDL-UDCA (n=5)	BDL-atRA (n=6)	BDL-UDCA&atRA (n=7)
Liver tissue (μmole/kg liver)	191.6±91.5	430.3±260.9	582.2±254.1	564.4±70.1	564±358.9
Bile cyst (mM)	N/A	15.79±5.14	16.30±4.44	23.00±8.00	10.25±8.72[4]
Bile cyst (μmole/kg body weight)	N/A	68.9±20.8	39.1±24.3[2]	35.6±24.7[2]	11.3±9.4[2,3]
Total hepatic bile salt (μmole/kg body weight)	5.58±2.67	94.79±19.92[1]	73.13±24.82[1]	61.78±24.68[1,2]	40.29±19.81[1,2,3]
Urine (mM)	0.02±0.02	1.22±1.15[1]	0.65±0.19[1]	0.51±0.68	0.52±0.41[1]
Bile acid pool size (μmole/kg body weight)	6.35±2.48	133.60±21.98[1]	112.49±28.94[1]	88.19±33.34[1,2]	74.47±25.32[1,2,3]

Note:

N/A, not applicable.

[1] p-value < 0.05 to Sham control

[2] to BDL-PBS control

[3] to UDCA treatment

[4] atRA treatment.